Russian Chemical Bulletin, International Edition, Vol. 63, No. 12, pp. 2585—2590, December, 2014

Full Articles

Quantum chemical simulation of the C—C bond cleavage in a propionic acid molecule on small palladium clusters

R. S. Shamsiev,* I. E. Sokolov, and V. R. Flid

M. V. Lomonosov Moscow State University of Fine Chemical Technologies,
86 prosp. Vernadskogo, 119571 Moscow, Russian Federation.
Fax: +7 (495) 434 8711. E-mail: Shamsiev.R@gmail.com

The C—C bond cleavage in a propionic acid molecule on the surface of Pd_n clusters (n = 4, 6, 8, 9) was simulated by the density functional theory with the PBE functional. Energetically preferable states of the metal clusters were found. Activation parameters of the cleavage process were calculated. The influence of the cluster size and the accessibility of Pd atoms for coordination on the activation parameters was determined.

Key words: density functional theory, PBE functional, palladium clusters, deoxygenation of carboxylic acids, C—C bond cleavage.

The continuous increase of energy use under conditions of increasing costs of traditional fuel resourses makes the production of hydrocarbon fuel from renewable raw plant materials very appealing. Additionally, data on the use of alternative fuel sources, such as biodiesel, demonstrate their advantages compared to oil.[1] The prospects of bioenergy encourage the development of new technologies of fuel production from renewable raw materials, design of efficient catalysts, and study of the mechanisms of the processes, which its production is based on. The reactions of catalytic decomposition of fatty acids, in particular their deoxygenation, are such processes.[2]

The main directions of the process of deoxygenation of fatty acids in the case of stearic acid are decarbonylation and decarboxylation:

$$C_{17}H_{35}COOH \rightarrow C_{17}H_{34} + CO + H_2O,$$

$$C_{17}H_{35}COOH \rightarrow C_{17}H_{36} + CO_2.$$

The reaction products are heptadecane, heptadecene, CO, CO_2, H_2O, as well as octadecane. Their amount and ratio depend on the reaction conditions. In the works,[3—6] the mechanism of these reactions was studied in the presence of metal catalysts, usually transition metals deposited on various substrates. Activity of the catalysts depends on the metal type. The most efficient are palladium catalysts.

Due to the labor-consuming character and methodical restrictions of detailed experimental study of the mechanism and the activation parameters of the reaction, it is reasonable to use a theoretical approach. Quantum chemical calculations[3] showed that the general and at the same time the rate-determining step for the two directions of deoxygenation is the C—C bond cleavage in the fatty acid molecule leading to the formation of the COOH species and the corresponding alkyl fragment. The goal of the present work is to calculate the activation parameters of

Published in Russian in *Izvestiya Akademii Nauk. Seriya Khimicheskaya,* No. 12, pp. 2585—2590, December, 2014.

this key stage, which ocurrs on the surface of model palladium clusters.

Calculation Methods

Calculations were performed in the framework of the scalar relativistic method of density functional theory (DFT) using the Priroda program.[7] An *ab initio* exchange correlation PBE functional[8] and a full-electron basis set[9] Л11 were used. For systems with open electron shells, the spin-polarized calculations were performed. Spin populations and atom charges were determined in agreement with the published procedure.[10]

The geometries of the structures were optimized with no symmetry restrictions. The types of found stationary points were determined based on analytically calculated second derivatives of energies and frequencies of normal vibrations. In order to check the correspondence of the found transition states (TS) to the local minima, calculations of the intrinsic reaction coordinate (IRC) were performed.

The simulation of the C—C bond cleavage was performed using the classical scheme. First, the structures with the COOH and C_2H_5 fragments on the surface of Pd_n clusters were optimized. Then, the calculations, for which the variable reaction coordinate was the distance between the C atoms of these fragments, were performed. After the analysis of the obtained energy profiles, starting TS structures were chosen, which were then optimized. In the last step of the simulation, the IRC was calculated and the structures corresponding to the reagents and the products of the propionic acid C—C bond cleavage were optimized.

The coordinates of the Pd atoms in clusters were not "frozen". The zero-point energies of vibrations and the thermodynamic characteristics were calculated in the rigid rotor and harmonic oscillator approximations taking into account the structure symmetries. The relative Gibbs energies were calculated at 298.15 K, as well as at 623.15 K, which corresponded to most of the experimental studies of fatty acid deoxygenations.

Quantum chemical calculations were performed using the calculation facilities of the M. V. Lomonosov Moscow State University super computer complex.

Results and Discussion

In order to simulate the C—C bond cleavage in a molecule of propionic acid, we chose Pd_4, Pd_6, Pd_8, and Pd_9 clusters. The energy characteristics of these models in various electron states with spin multiplicity $M = 1, 3, 5$, and 7 are given in Table 1. As it can be seen from the Table 1, the triplet state is the most energetically favorable for all palladium clusters. However, for Pd_8 and Pd_9 clusters the relative Gibbs energies at $T = 623.15$ K for states with multiplicity 3 and 5 are quite close. Due to this, from here we use only Pd_n clusters with $M = 3$ and additionally Pd_8 and Pd_9 with $M = 5$. The optimized cluster structures with $M = 3$ are given in Fig. 1.

From the calculations it can be seen that the Pd_4 cluster is a distorted tetrahedron with D_{2d} symmetry and 2.58 and 2.64 Å sides. All Pd atoms in this cluster are equivalent, which is shown by the spin populations given in Table 2. Each Pd atom in the Pd_4 cluster is bonded to three others (see Fig. 1).

Table 1. Relative energies not including (ΔE) and including the zero-point energies of vibrations (ΔE_0) and relative Gibbs energies (ΔG°) (kJ mol^{-1}) for Pd_n clusters with spin multiplicity M

Cluster	M	ΔE	ΔE_0	ΔG°	
				298 K	623 K
Pd_4	1	0.00	0.00	0.00	0.00
	3	−42.21	−42.28	−42.52	−42.77
	5	77.70	78.03	79.05	80.09
Pd_6	1	0.00	0.00	0.00	0.00
	3	−6.66	−6.57	−6.59	−6.64
	5	59.58	58.92	55.40	51.63
	7	132.01	131.63	129.17	126.51
Pd_8	1	0.00	0.00	0.00	0.00
	3	−21.53	−21.51	−21.11	−21.39
	5	−19.61	−19.59	−19.48	−19.37
	7	28.21	28.10	27.31	26.44
Pd_9	1	0.00	0.00	0.00	0.00
	3	−20.73	−20.96	−22.67	−24.52
	5	−18.84	−19.46	−22.16	−25.00
	7	23.80	23.09	18.82	14.24

The Pd_6 structure is a tetragonal bipyramid with D_{4h} symmetry and 2.61 and 2.70 Å sides. Two groups of atoms can be identified in this cluster: in the first group are the Pd(3) and Pd(4) atoms located in the vertices of the bipyramid, and in the second group are the other four atoms (see Fig. 1). The non-equivalence of these atoms is indicated by the spin populations of 0.14 and 0.43 a.u., respectively (see Table 2). At that, the coordination number (CN) for each of the six Pd atoms is the same and equal to four.

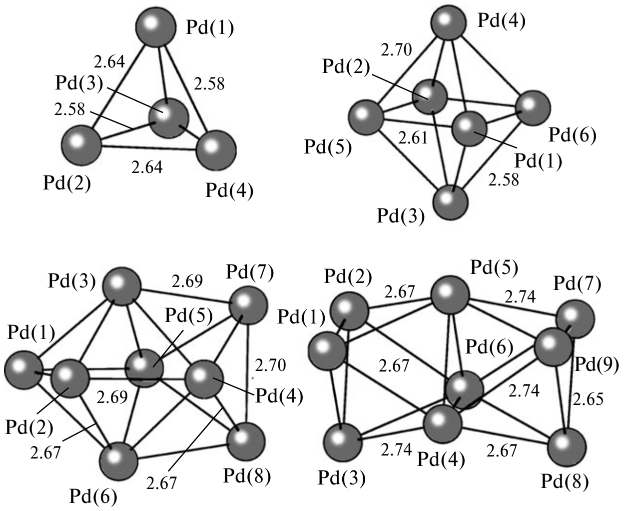

Fig. 1. Optimized structures of Pd_n ($n = 4, 6, 8, 9$) clusters. Here and further on, the interatomic distances are given in Å.

Table 2. Spin populations (a.u.) of the atoms in Pd_n clusters with spin multiplicity M

Atom*	Pd_4 ($M = 3$)	Pd_6 ($M = 3$)	Pd_8 ($M = 3$)	Pd_8 ($M = 5$)	Pd_9 ($M = 3$)	Pd_9 ($M = 5$)
1	0.50	0.43	0.22	0.52	0.25	0.37
2	0.50	0.43	0.22	0.52	0.08	0.37
3	0.50	0.14	0.28	0.48	0.27	0.37
4	0.50	0.14	0.28	0.48	0.43	0.59
5	—	0.43	0.28	0.48	−0.06	0.59
6	—	0.43	0.28	0.48	0.43	0.59
7	—	—	0.22	0.52	0.24	0.37
8	—	—	0.22	0.52	0.27	0.37
9	—	—	—	—	0.08	0.37

* The atom numbering is given in Fig. 1.

The Pd_8 cluster is formed by the addition of two atoms to the Pd_6 cluster. The optimized structure of this cluster corresponds to D_{2d} symmetry, and two groups of atoms can be identified in it, as well: Pd(1), Pd(2), Pd(7), Pd(8) with CN = 4 and Pd(3), Pd(4), Pd(5), Pd(6) with CN = 5. The spin populations of each atom in these groups at $M = 3$ are equal to 0.22 and 0.28 a.u., respectively (see Table 2). The Pd—Pd bond lengths are in the interval of 2.65—2.73 Å.

The Pd_9 cluster with C_{2v} symmerty is built in two layers: one layer consists of five Pd atoms, and the other layer consists of four Pd atoms. Such a configuration is chosen due to it having the most surface Pd atoms. In this case the following two groups of atoms can be identified: Pd(1), Pd(2), Pd(3), Pd(7), Pd(8), Pd(9) with CN = 4 and Pd(4), Pd(5), Pd(6) with CN = 6. The spin populations of these atoms for $M = 5$ are equal to 0.37 and 0.59 a.u., respectively (see Table 2). The average bond lengths in the studied clusters are in good agreement with literature data.[11]

The activation parameters of the TSs of the propionic acid C—C bond cleavage on Pd_n clusters are given in Table 3. Since the four atoms in a Pd_4 cluster are equivalent from the point of view of spin populations and coordination number, only one TS **1** is found for this cluster, which is shown in Fig. 2.

The optimization of the TS structures for the Pd_6 cluster, when the C—C cleavage occurs on Pd(1) and Pd(4) atoms (TSs **2** and **3** in Fig. 3, respectively), which belong to different groups of equivalent atoms, showed the minimal geometric and energetic differences. In this case, a noticeable difference in the spin populations of Pd(1) and Pd(4) atoms in the Pd_6 cluster (see Table 2) does not considerably affect the energetics of the C—C bond cleavage stage (see $\Delta E^{\neq}$ and $\Delta E^{\neq}_0$ in Table 3). Ttansition state **4**

Table 3. Activation parameters of the propionic acid C—C bond cleavage on Pd_n clusters with spin multiplicity M

Cluster	Structure	M	$\Delta E^{\neq}$	$\Delta E^{\neq}_0$	$\Delta^{\neq}H^\circ_T$		$-\Delta^{\neq}S^\circ_T$		$\Delta^{\neq}G^\circ_T$	
					298 K	623 K	298 K	623 K	298 K	623 K
Pd_4	**1**	3	41.50	33.93	27.48	32.49	151.11	139.65	72.54	119.52
Pd_6	**2**	3	40.46	31.24	23.97	29.24	132.04	119.97	63.34	104.00
	3	3	40.54	31.37	24.16	29.41	113.69	101.67	58.06	92.77
	4	3	33.09	23.78	16.38	21.68	133.31	121.16	56.13	97.19
	5	3	13.23	4.92	−2.72	2.41	167.08	158.74	47.75	101.33
Pd_8	**5**	5	52.55	44.20	36.90	42.01	160.77	149.14	84.84	134.94
	6	3	25.17	15.36	6.98	12.50	154.85	145.58	53.81	103.22
	7	3	34.27	25.60	17.69	22.89	164.70	156.22	67.46	120.23
	8	3	23.04	15.03	7.45	12.51	170.61	162.45	58.98	113.75
	8	5	22.74	14.69	7.36	12.38	166.26	154.83	56.93	108.87
Pd_9	**9**	5	34.31	25.32	17.18	22.55	176.55	164.26	69.81	124.91
	10	3	36.75	28.82	21.56	26.65	178.36	166.76	74.74	130.56
	10	5	29.55	21.87	14.71	19.74	180.33	168.87	68.47	124.97
	11	3	24.76	16.07	7.87	13.01	180.44	168.75	61.67	118.17
	11	5	21.24	12.76	4.79	9.96	180.53	168.76	58.62	115.12

Note. Energies not including ($\Delta E^{\neq}$) and including the zero-point energies of vibrations ($\Delta E^{\neq}_0$), enthalpies ($\Delta^{\neq}H^\circ$), free energies ($\Delta^{\neq}G^\circ$) (kJ mol^{-1}), and entropies ($\Delta^{\neq}S^\circ$/J mol^{-1} K^{-1}) of the transition states relative to the isolated EtCOOH and Pd_n species.

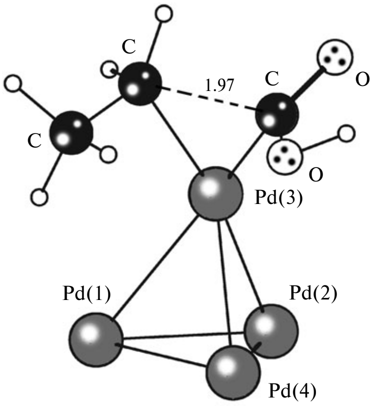

1

Fig. 2. Optimized structure of the TS **1** of the propionic acid C—C bond cleavage on a Pd_4 cluster.

structure **4** (see Fig. 3) was obtained by changing the positions of the ethyl fragment from *cis* to *trans* relative to the hydroxy group of the COOH fragment. Such a TS "modification" did not noticeably affect the cleavage stage energetics: the difference in the free activation energies $\Delta^{\neq}G^{\circ}$ for structures **2** and **4** is less than 5 kJ mol^{-1} (see Table 3).

For the Pd_8 cluster, we found four TSs, in which the C—C bond cleavage of the propionic acid molecule occurs on the Pd(1) (TSs **5** and **6**, Fig. 4) and the Pd(3) (TSs **7** and **8**, Fig. 4) atoms belonging to different groups of equivalent atoms. The TSs **5** and **6** differ by the position of the ethyl fragment relative to the COOH group. This practically does not affect the free activation energy $\Delta^{\neq}G^{\circ}$ (see Table 3). Transition states **7** and **8** (see Fig. 4) have the same geometric differences, but the energy difference $\Delta^{\neq}G^{\circ}$ is more noticeable (see Table 3).

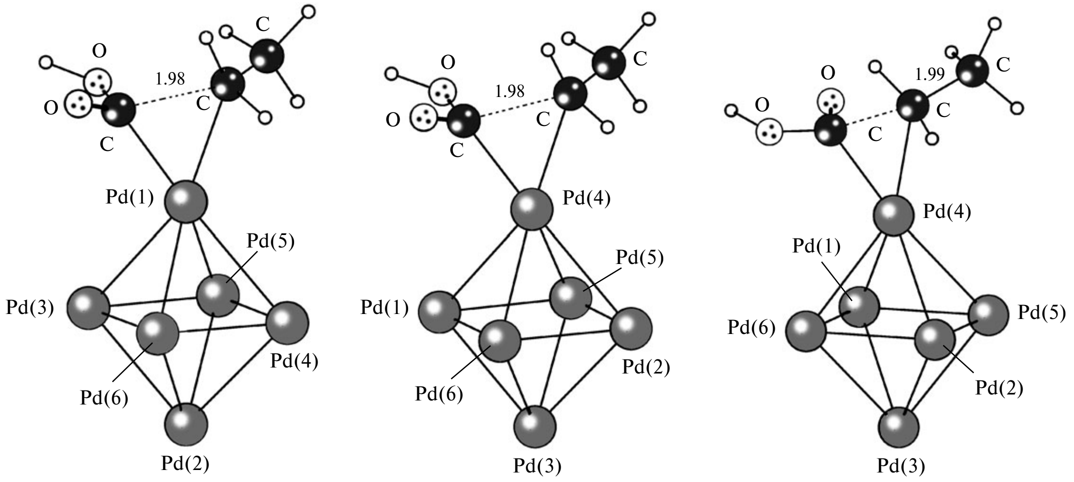

2 **3** **4**

Fig. 3. Optimized structures of the TSs **2**—**4** of the propionic acid C—C bond cleavage on a Pd_6 cluster.

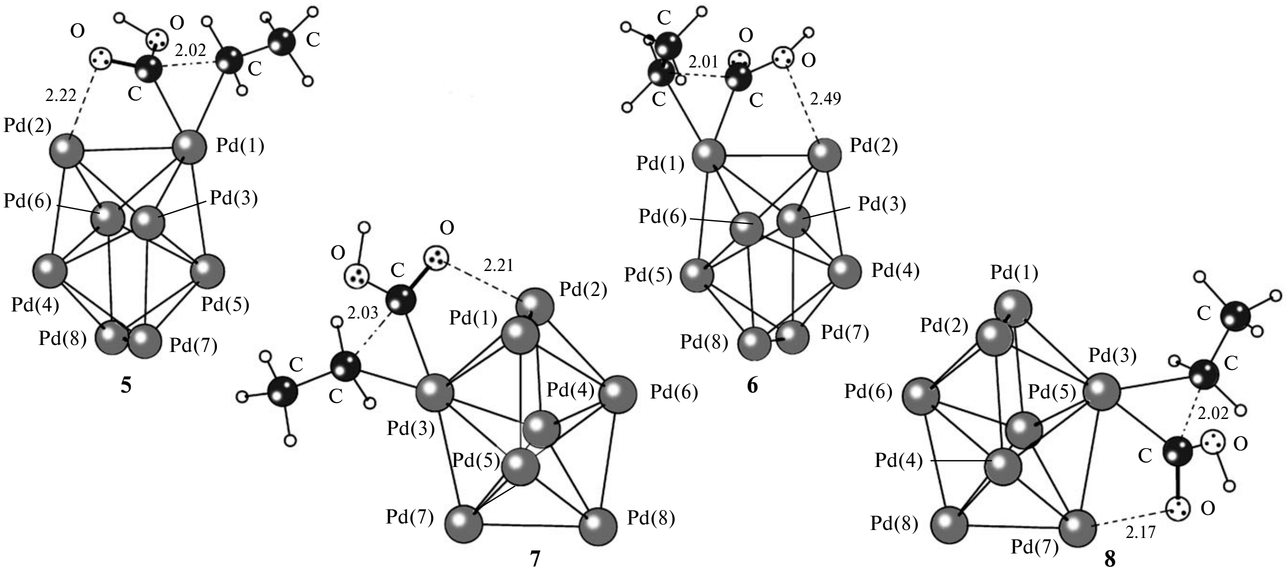

5 **7** **6** **8**

Fig. 4. Optimized structures of the TSs **5**—**8** of the propionic acid C—C bond cleavage on a Pd_8 cluster.

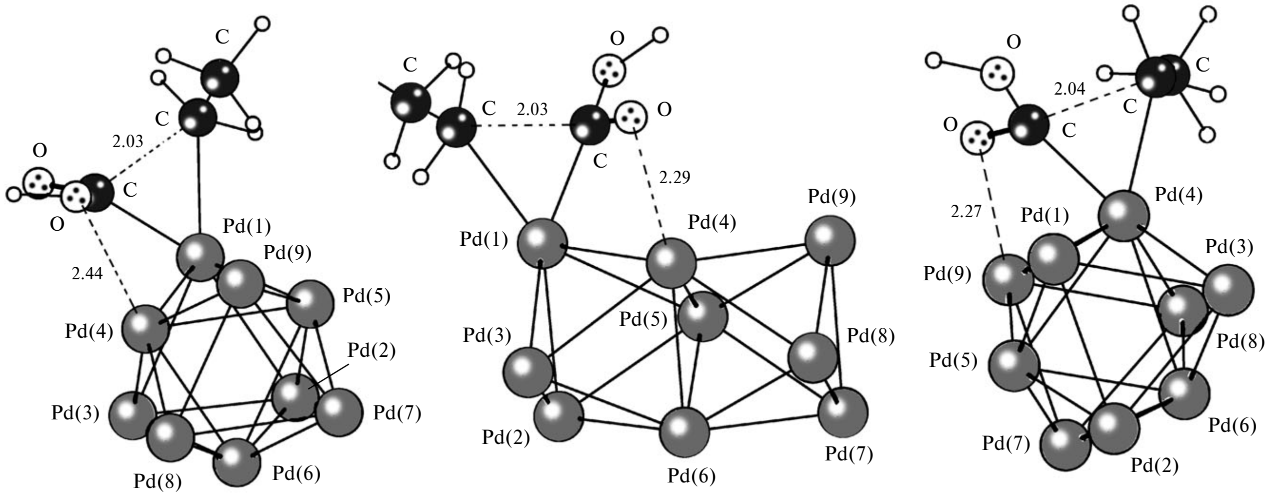

9 **10** **11**

Fig. 5. Optimized structures of the TSs **9**—**11** of the propionic acid C—C bond cleavage on a Pd_9 cluster.

Transition states **5** and **8** with multiplicity 5 were also calculated. While, for TS **8**, the change in multiplicity led to a small decrease in the free activation energy $\Delta^{\neq}G^{\circ}$, for TS **5** it led to its noticeable increase (see Table 3).

Three TSs for the C—C bond cleavage stage on the Pd_9 cluster are given in Fig. 5. Transition states **9** and **10** correspond to the process on the Pd(1) atom with CN = 4 and differ by the position of the COOH fragment: in TS **9** the O atom of the OH group is closer to the surface of the cluster (2.44 Å), while in TS **10** another O atom of the COOH group is closer to it (2.29 Å). These features do not lead to a noticeable difference in the activation barriers. In TS **11**, the C—C bond cleavage occurs on the Pd(4) atom with CN = 6. The differences in the energetic parameters of TSs **10** and **11** with multiplicity 3 and 5 are small (see Table 3). Note that we were not able to detect a TS, in which the C—C bond cleavage proceeded on two or more Pd atoms.

The dependencies of the free activation energy on the coordination number, spin population, and charge on the reacting Pd atom, where the C—C bond is cleaved, are given in Figs 6—8. From these figures it can be seen that these dependencies are ambiguous. For example, while for Pd_8 an increase in the CN of the Pd atom leads to an increase in $\Delta^{\neq}G^{\circ}_{623}$, for Pd_9 it results in a descrease in $\Delta^{\neq}G^{\circ}_{623}$ (see Fig. 6). In general, for the same CN (equal to four, for example) an increase in cluster size leads to a considerable increase in the activation barrier. An increase in the spin population (see Fig. 7) or atom charge (see Fig. 8) leads to an increase in the activation barrier $\Delta^{\neq}G^{\circ}_{623}$ for Pd_6 and Pd_8 clusters, and for Pd_9, to its decrease.

In conclusion, the quantum chemical study of the C—C bond cleavage stage in a propionic acid molecule on Pd_n clusters (n = 4, 6, 8, 9) showed that the accessibility for coordination and spin populations of the reacting atoms

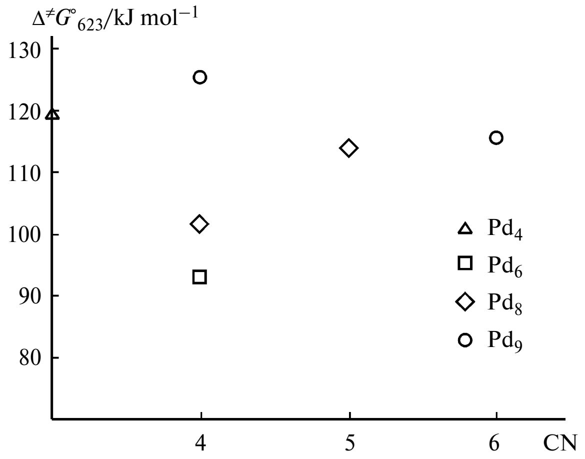

Fig. 6. Dependence of the free activation energy on the coordination number of the Pd atom for the Pd_n + C_2H_5COOH system.

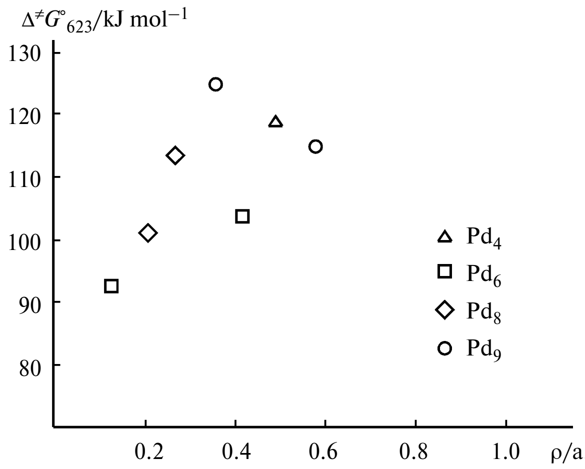

Fig. 7. Dependence of the free activation energy on the spin population (ρ) of the Pd atom for the Pd_n + C_2H_5COOH system.

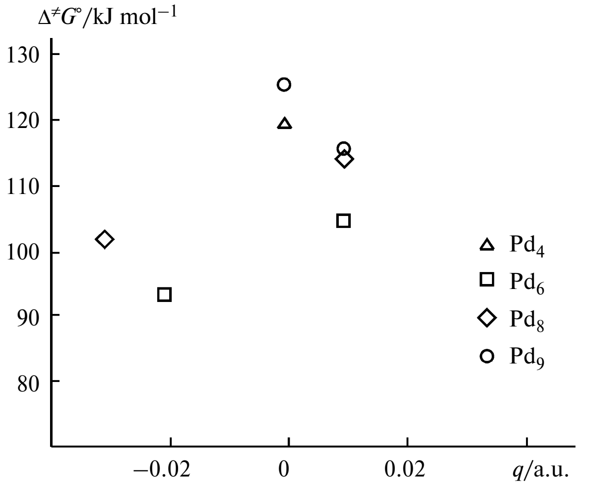

Fig. 8. Dependence of the free activation energy on the charge (q) of the Pd atom for the $Pd_n + C_2H_5COOH$ system.

in palladium clusters affect activation barriers considerably and in different ways. For the same coordination number of the reacting Pd atoms, an increase in the cluster size leads to the increases in the free activation energy. For all studied clusters, the C—C bond cleavage of the acid molecule proceeds by a three-centered mechanism involving only one Pd atom.

This work was financially supported by the Ministry of Education and Science of the Russian Federation (State Assignment No. 2014/114).

References

1. T. N. Kalnes, T. Marker, D. R. Shonnard, K. P. Koers, *Int. J. Chem. React. Eng.*, 2007, **5**, 48.
2. A. S. Berenblyum, T. A. Podoplelova, R. S. Shamsiev, E. A. Katsman, V. Ya. Danyushevsky, V. R. Flid, *Catalysis in Industry* (*Engl. Transl.*), 2012, **4**, 209 [*Kataliz v Promyshlennosti*, 2012, **4**, 84].
3. A. S. Berenblyum, T. A. Podoplelova, R. S. Shamsiev, E. A. Katsman, V. Ya. Danyushevsky, *Petrol. Chem.* (*Engl. Transl.*), 2011, **51**, 336 [*Neftekhimiya,* 2011, **51**, 342].
4. A. S. Berenblyum, T. A. Podoplelova, E. A. Katsman, R. S. Shamsiev, V. Ya. Danyushevsky, *Kinet. Catal.* (*Engl. Transl.*), 2012, **53**, 595 [*Kinet. Katal.*, 2012, **53**, 634].
5. A. S. Berenblyum, R. S. Shamsiev, T. A. Podoplelova, V. Ya. Danyushevsky, *Russ. J. Phys. Chem.* (*Engl. Transl.*), 2012, **86**, 1199 [*Zh. Fiz. Khim.*, 2012, **86**, 1340].
6. A. S. Berenblyum, V. Ya. Danyushevsky, E. A. Katsman, R. S. Shamsiev, V. R. Flid, *Petrol. Chem.* (*Engl. Transl.*), 2013, **53**, 362 [*Neftekhimiya*, 2013, **53**, 408].
7. D. N. Laikov, *Chem. Phys. Lett.*, 1997, **281**, 151.
8. J. P. Perdew, K. Burke, M. Ernzerhof, *Phys. Rev. Lett.*, 1996, **77**, 3865.
9. D. N. Laikov, *Chem. Phys. Lett.*, 2005, **416**, 116.
10. F. L. Hirshfeld, *Theor. Chim. Acta*, 1977, **44**, 129.
11. S. Krüger, S. Vent, F. Nörtemann, M. Staufer, N. Rösch, *J. Chem. Phys.*, 2001, **115**, 2082.

Received July 17, 2014;
in revised form November 10, 2014